International Journal of Multiphase Flow 34 (2008) 1058–1066

Contents lists available at ScienceDirect

International Journal of Multiphase Flow

journal homepage: www.elsevier.com/locate/ijmulflow

Subcooled pool boiling of water on a downward-facing stainless steel disk in a gap

G.H. Su [a,*], Y.W. Wu [a], K. Sugiyama [b,1]

[a] State Key laboratory of Multiphase Flow in Power Engineering, Department of Nuclear Science and Technology, Xi'an Jiaotong University, Xi'an City 710049, China
[b] Faculty of Engineering, Hokkaido University, Kita 13 Jo, Nishi 8 Chome, Kita-Ku, Sapporo 060-8628, Japan

ARTICLE INFO

Article history:
Received 25 September 2007
Received in revised form 8 June 2008
Accepted 6 July 2008
Available online 31 July 2008

ABSTRACT

Pool boiling is experimentally studied on a relatively large downward-facing surface with heated stainless steel disk diameters of D = 100 and 300 mm in confined space at atmospheric pressure using water as the working fluid. The bulk working fluid is subcooled. The gap size s can be adjusted to 10, 15 and 20 mm for D = 100 mm and 0.9–77 mm for D = 300 mm. We found that pool boiling under the present condition is far weaker than that occurring on an upward-facing surface. Furthermore, we found that the larger the diameter of the stainless steel plate, the weaker the pool boiling heat transfer. The heat transfer rate may be predicted by the Kutateladze correlation for s > 20 mm and by its modified form for s < 20 mm for both D = 100 and D = 300 mm. Two different typical bubble circulation motions are found. Type I motion occurs with a probability of 90.9% and type II occurs with a probability of 9.1% according to the statistical calculations. Most coalesced bubble diameters are from 90 to 100 mm for D = 100 mm and from 100 to 200 mm for D = 300 mm.

1. Introduction

The confined boiling heat transfer on downward-facing surfaces has been investigated since the TMI-2 accident. Many studies indicated that a gap between the lower pressure vessel head and debris formed and cooled the lower pressure vessel head via an unknown mechanism according to a justified scenario (Wolf et al., 1994). The design of the advanced light water reactor, and its proper management to prevent melt through of the reactor vessel in the event of a core meltdown accident, require clarification of the boiling heat transfer on the outer surface of the lower head to remove decay heat from the molten core. The boiling heat transfer on the downward-facing surfaces becomes important in these cases.

Due to buoyancy, convective heat transfer occurs with increasing heat flux on a surface initially in thermal equilibrium with the host working fluid in a subcooled pool. Nucleate boiling starts by further increasing the surface temperature or heat flux and bubbles appear randomly on the heated surface. A number of experimental, theoretical, and numerical studies on boiling heat transfer have been performed since the incident (Phanikumar and Mahajan, 1998; Bonjour and Lallemand, 1998, 2001; Radziemska and Lewandowski, 2001; Yoon et al., 2001; Hetsroni et al., 2002; Nomura et al., 2002; Su et al., 2002a,b, Su and Sugiyama, 2007; Kim and Jeong, 2006; Kim and Kim, 2006; Lee et al., 2007; Prakash Narayan et al., 2008). Many experiments (Yao and Chang, 1983; Nishigawa et al., 1984; Carrica et al., 1995; El-genk and Glebov, 1995, 1996; El-genk and Gao, 1999; Yang et al., 1997; Kim and Suh, 2003; Lee et al., 2003; Kim et al., 2005, 2006) have demonstrated the differences in boiling heat transfer for vertical, inclined, and horizontal heated surfaces. The characteristics of heat transfer for upward-facing and downward-facing pool boiling on a horizontal heated surface are different because the vapor generated in boiling cannot readily move from the hot surface to depart from the edge of the downward-facing heated surface. Thus, it is easy to form a coalescence bubble on a downward-facing surface. The coalesced bubbles grow on the heated surface before their departure from the edge.

Haddad and Cheung (1998) studied the steady-state subcooled nucleate boiling on a downward-facing hemispherical aluminum surface and found that subcooling had very little effect on the nucleate boiling curve in the high heat flux regime dominated by latent heat transport. On the other hand, a relatively large effect of subcooling was observed in the low heat flux regime where sensible heat transport was important. This effect of subcooling is the same as that observed on an upward-facing surface. In the high heat flux region, boiling in the bottom center region of a vessel with a curved downward-facing surface was cyclic and consisted of four phases, i.e., a liquid heating phase, a bubble nucleation and growth phase, a bubble coalescence phase, and a large vapor mass ejection phase.

Katto et al. (1977) investigated the nucleate boiling of water in a confined space between two horizontal parallel disks with different gaps from 0.1 to 2 mm, where one disk was an upward-facing

* Corresponding author. Tel./fax: +86 29 82663401.
E-mail addresses: ghsu@mail.xjtu.edu.cn (G.H. Su), k-sugi@eng.hokudai.ac.jp (K. Sugiyama).
[1] Tel./fax: +81 11 7067842.

0301-9322/$ - see front matter © 2008 Elsevier Ltd. All rights reserved.
doi:10.1016/j.ijmultiphaseflow.2008.07.004

heated surface and the other was unheated. A marked decrease in the heat transfer coefficient was observed when the gap size was reduced to $s = 0.1$ mm, corresponding to a Bond number of 0.04.

Bond number, Bo, is used to express the confinement level for several geometrical chambers, and is defined by

$$Bo = s\sqrt{g(\rho_f - \rho_g)/\sigma} \quad (1)$$

where s is the gap size and is the characteristic dimension of the confined space. σ represents the surface tension, ρ_f and ρ_g are the saturated liquid density and saturated vapor density, respectively, and g is the acceleration of gravity. $\sqrt{\sigma/(\rho_f - \rho_g)g}$ is the departure diameter of the isolated bubble, which is assumed to be the capillary length as denoted by

$$L = \sqrt{\sigma/(\rho_f - \rho_g)g} \quad (2)$$

Under an atmospheric pressure condition, the capillary length is about 2.5 mm.

Thus, the Bond number is a ratio of the gap size to the capillary length, and may also be expressed as

$$Bo = s/L \quad (3)$$

Chu et al. (1997) observed the quenching of either flat or curved downward facing aluminum surfaces with 61 cm diameters to simulate and assess the ex-vessel boiling process for in-vessel core retention. The experimental masses were heated to an elevated temperature between 160 and 330 °C, and then plunged into a pool of water at saturation. The boiling curves were obtained where the critical heat flux was found to be approximately 0.5 MW/m^2.

Passos et al. (2004) studied the confined boiling of FC72 and FC87 on a downward-facing heating copper disk (diameter of 12 mm and thickness of 2 mm) at atmospheric pressure. At saturated boiling and low heat flux ($\leqslant$45 kW/m^2), a decrease in the distance between plates enhances boiling. The results for subcooled boiling show that the heat transfer coefficient decreases with a reduction in the distance between the plates.

El-genk and Glebov (1995) performed quenching experiments to investigate the effects of wall thickness on pool boiling from downward curved surfaces using water as the working fluid. Local and average pool boiling curves were obtained under saturation and subcooling conditions.

The previous studies on boiling heat transfers on downward-facing surfaces are summarized in Table 1.

As described above, most previous studies on pool boiling heat transfer on downward-facing surfaces have been done for curved surfaces. Although there is limited open literature on pool boiling heat transfer on the horizontal downward-facing surfaces, there is a lack of data for understanding the mechanisms for and differences between upward- and downward-facing pool boiling. In particular, data are required to derive the empirical relationship for pool boiling heat transfer for horizontal downward-facing surfaces.

In the present study, pool boiling experiments have been conducted to examine the boiling process on a downward facing heated surface using stainless steel flat blocks with 100 and 300 mm diameters under different gap size conditions.

2. Experiments

2.1. Experimental apparatus

Tests are performed in a thin pool using water as working fluid at atmospheric pressure. The experimental apparatus (Fig. 1) consists of a test section, data acquisition system, and an auxiliary system that is used to control the level of the working fluid. The test section has two stainless steel blocks, one with a diameter of 100 mm and thickness of 30 mm and the other with a diameter of 300 mm and a thickness of 30 mm. The blocks are placed in turn at the center of an acrylic box with a height of 150 mm, length of 900 mm and width of 750 mm. The acrylic box is significantly larger than each heated block. If a heated block has a diameter almost equal to the length of the box, the difference between the water temperatures under and around the heated block are very small and the wave on the water surface due to the escape and decomposition of bubbles very strong. To ensure boiling heat transfer occurs on the downward-facing bottom surface, thermal insulation is used on the top surface and around the sides of the heated block. The thermal insulator is then isolated from the water by a thin stainless steel plate to keep the thermal insulator dry.

The gap size between the bottom surface of the stainless steel plate and the base of the acrylic vessel is adjustable by lifting the test section. In this study, the gap sizes are 10, 15 and 20 mm for the test section with a 100 mm diameter and 0.9, 2.2, 2.6, 3.0, 3.2, 5.0, 7.0, 10.0, 13.0, 15.6, 19.5, 25.0, 36.0, 51.0 and 77 mm for the test section with a 300 mm diameter. When the gap size is less than 7 mm, the bottom surface of the acrylic vessel is easily deformed by the impact of the saturated fluid. Thus, there is an addi-

Table 1
State-of-the-art of the boiling heat transfer on a downward-facing surface

References	Experimental method	Type of surface	Main findings
El-genk and Glebov (1995)	Quenching water	Curved copper	Effects of wall thickness on pool boiling
El-genk and Glebov (1996)	Quenching water	Curved copper	Local and surface average Nusselt numbers were correlated in terms of the Rayleigh and Jacob numbers
Yang et al. (1997)	Direct joule heating water (slightly subcooled)	Plate stainless steel	Effects of surface inclination angle and size on the pool boiling CHF
Haddad and Cheung (1998)	Steady-state heating water	Aluminum hemispherical	Subcooling has very little effect on nucleate boiling curve in the high heat flux regime; a relatively large effect of subcooling is observed in the low heat flux regime
Cheung et al. (1999)			A scaling law was established
Ahmed and Carey (1999)	Heating water/2-propanol mixture	Upward-facing and downward-facing heater surface	Boiling curves and CHF at different conditions
El-genk and Bostanci (2003)	HFE-7100	Plate copper	Combined effects of subcooling and surface orientation on pool boiling
Yang et al. (2005)	Steady-state boiling	Coated hemispherical downward-facing surface	Compared to the corresponding data without coatings, the boiling curves for the coated vessels were found to shift upward and to the right
Present study	Steady-state water boiling	Plate in a gap	Derived a correlation to predict downward-facing boiling heat transfer, two kinds of bubble circulation motions were found

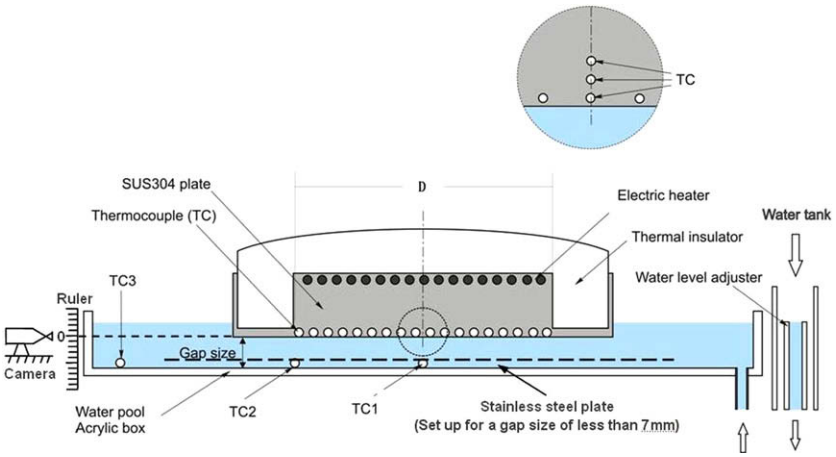

Fig. 1. Experimental apparatus.

tional error in the gap size measurement. To eliminate this error, an additional stainless steel plate is installed between the heated surface and base of the acrylic vessel to produce the required gap size. This means the gap is the space between the heated block and the stainless steel plate when the gap size is smaller than 7 mm. To record the bubble behavior using a digital video camera under the acrylic vessel, no additional stainless steel plate is employed when the gap size is larger than 7 mm.

The test section is heated by three electric heaters. Each heater has a maximum power of 3.12 kW, diameter of 4.8 mm and length of 2.0 m. K-type NiCr–NiSi thermocouples with diameters of 1.6 mm are employed to measure the temperature. Their maximum uncertainty is ±0.5 °C. There are a total of 37 thermocouples that measure the temperature at different locations (Fig. 1) of the test section, with 28 located near the heated surface. There are three sets of three vertically aligned thermocouples, with the thermocouples at immersion depths of 21.8, 24.8 and 28.2 mm as shown in Fig. 1, for the evaluation of heat flux in the vertical direction. Water temperatures below the center and edge of the block, TC1 and TC2, and near the edge of the acrylic box, TC3, are also measured by three thermocouples. All data are recorded by the acquisition system.

2.2. Data reduction

In the present study, it is very difficult to determine the subcooling. It is known that when pool boiling occurs on a surface facing upward, micro-natural circulation occurs. The subcooling is determined by the inlet temperature of this flow, which can be measured by a thermocouple TC. When the pool boiling occurs on the heated surface facing downward in the confined space, micro-natural circulation may not easily form in the limited space. Thus, there is no obvious inlet for the micro-circulation. The heat mainly transfers by liquid conduction from the center of the gap to the peripheral liquid except for the escape of bubbles. The temperature measured by thermocouple TC2, as shown in Fig. 1, can of course be used to determine the subcooling. However, when the gap size is less than 7 mm, the fluid is saturated although the temperature measured by TC3 is for a subcooled state. Thus, to consider the effect of subcooling on pool boiling in this study, the temperature measured by thermocouple TC3 is used to determine the subcooling.

For pool boiling on a downward-facing surface in a gap there are two important physical parameters that could significantly affect the nucleate boiling heat transfer and the critical heat flux. These two parameters are the diameter of the downward-facing surface and the gap size, s. While the gap size is varied in the present experiments, the size of the heating surface is not. That is, this paper employs a downward-facing surface with a fixed diameter, D, of 100 or 300 mm for all boiling experiments.

For downward-facing boiling in a gap, the shape of the vapor bubbles could be substantially different from spherical. Depending on the gap size, diameter of the heating surface, and heat flux level, the vapor bubbles could be highly elongated, similar to a pancake. For elongated bubbles, there are two characteristic length scales, i.e., the bubble width (horizontal direction) and the bubble height (vertical direction). The bubble width may be strongly influenced by the diameter of the heated surface, and could be of the order of the diameter of the heating surface if the nucleation site is at the center of the surface. Conversely, the bubble height may be limited to the gap size when the gap size is small. In our experiments, we used a high-speed digital camera to try to obtain the maximum height of the flattened bubble as shown in Fig. 1, but the videos were not clear enough to distinguish the bubble because of the distance between the heated plate and edge of the acrylic box and the disturbance of bubbles. Thus, we adopted a method of visual observation. According to our observation, the maximum height of the flattened bubble is approximately 5 mm if the gap size is larger than 5 mm. That is to say, the bubble height will be same as the gap size when the gap size is smaller than 5 mm; otherwise, it will be 5 mm. The width of the bubble is more important than the height because it directly affects the area of the heated surface covered by the bubble. Therefore, the characteristic length of the bubbles is selected as the width or diameter of the bubbles.

The bottom wall surface temperatures may be calculated according to the three temperatures measured in the vertical direction as shown in Fig. 1 by quadratic interpolation. The heat flux may then be obtained using the conduction law according to the temperature difference in the heated block. After the heat flux and wall temperature are found, the boiling curve can be plotted to initially show the experimental data.

Repeatability experiments were conducted on different days under the same experimental conditions to test the reliability of the experimental data. The data demonstrate good repeatability of the experimental results with almost the same boiling curves.

3. Results and discussion

3.1. The effect of the gap size on subcooled pool boiling

Fig. 2 shows the effect of the gap size on the boiling curves when D = 300 mm. For gap sizes s = 0.9 and 3.0 mm, when the heat

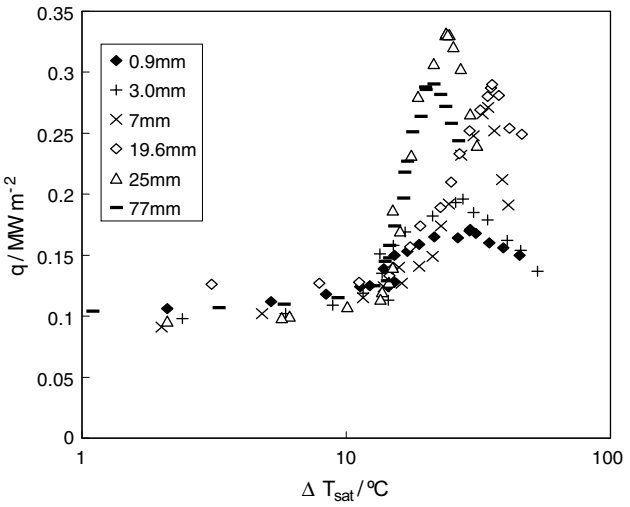

Fig. 2. Comparison of boiling curves for different gap sizes.

flux is smaller than 0.16 MW/m^2, the wall superheat, $\Delta T_{sat} = T_W - T_{sat}$, in which T_W is the wall temperature and T_{sat} is the saturated temperature, is less than that for $s = 7$ mm because the boiling curves for $s = 0.9$ and 3.0 mm are much steeper than that for $s = 7$ mm. That is to say, for the same heat flux, the results of $s = 0.9$ and 3 mm show enhanced boiling. As discussed above, the maximum height of the flattened bubble is approximately 5 mm, which is twice the capillary length of about 2.5 mm. When the gap size is smaller than 5 mm, the squeezing effect of the bubbles in the gap becomes more important due to the gap being narrower than the thickness of the bubble. Therefore, the heat transfers for $s = 0.9$ and 3 mm are confined while that for $s = 7$ mm tends to be unconfined. When the heat flux is larger than 0.16 MW/m^2, the boiling curves for $s = 0.9$ and 3.0 mm tend to be flatter than those in relative lower heat flux, and the increase in the wall superheat or the increase in the wall temperature reduces the enhancement of the boiling. This phenomenon may be explained by the evaporation and conduction of liquid film between the flat bubble and the heating wall. When the heat flux is smaller than 0.16 MW/m^2, the influence of the evaporation is dominant while the conduction of the liquid film is secondary. When the gap size is smaller than 5 mm, the deformation of the bubble increases the area of the liquid film and the evaporation effect increases. This effect pushes the efficient heat transfer from the heated wall to the liquid in the boiling process. In the relatively higher heat flux region, that is, where the heat flux is larger than 0.16 MW/m^2, the effect of evaporation becomes weak because more bubbles are generated and coalesce to form a huge bubble because the bubbles cannot immediately escape to the liquid pool. Thus, the residence time of the bubbles or huge bubble in the gap increases.

In the region where the gap size is larger than 5 mm but smaller than 20 mm, there are some differences between the boiling curves for different gap sizes. When the heat flux is low (less than approximately 0.2 MW/m^2), due to the strong disturbance in the larger gap size, the wall superheat for $s = 19$ mm is smaller than that for $s = 7$ mm for the same heat flux. When the heat flux is larger than 0.2 MW/m^2, the bubbles coalesce. The effect of the disturbance region tends to be weak, thus, the boiling curves for $s = 7$ and 19.6 mm are identical.

When the gap size is larger than 20 mm, the nucleate boiling curves for $s = 25$ and 77 mm are identical. According to our observation, the strong disturbance caused by the escaping bubbles may reach a depth of approximately 20 mm. When the depth is even deeper, although there is still a disturbance, it is far weaker and there is no confinement effect in this case.

Therefore, there is a transition region from the confined space to the unconfined space. The gap size of the transition region is from 5 to 20 mm. The boiling curve is close to that of the unconfined case, but there are also partial effects of confinement. Thus, this region should strictly be referred to as a semi-confined region.

In the unconfined region, the heat transfers for $s = 25$ and 77 mm are stronger than those for the confined or semi-confined gaps. This means that for the same heat flux, the wall superheat or wall temperature is smaller for unconfined space than for the confined gap. Thus, the gap size has no influence on the nucleate boiling curve. The fact that the nucleate boiling curves for $s = 25$ and 77 mm are identical indicate that the subcooling has no effect on the boiling curve because the subcooling for $s = 25$ mm is not the same as that for $s = 77$ mm.

It is worth noting that the above clarification of the confined, semi-confined and unconfined gaps is only suitable for the heated plate with a diameter of 300 mm. The experimental study for the heated circular plate with a diameter of 100 mm is only carried out for gap sizes of 10, 15 and 20 mm. Thus there are insufficient experimental data to strictly identify the confined, semi-confined and unconfined regions.

3.2. Developed empirical correlation

Fig. 3(a) and (b) presents the comparisons between the present experimental pool boiling data and the results of typical well known correlations (Kutateladze, 1952; Nishigawa and Fujita, 1977; Rohsenow, 1952; Stephan and Abdelsalam, 1980) and experimental data for an upward-facing surface (Ono and Sakashita, 2004) for an unconfined space. It is known that empirical or semi-empirical correlations for upward pool boiling do not agree well because they were developed based on different databases. Furthermore, they are not consistent with other experimental data. There are great differences between our experimental data and the Rohsenow and Stephan correlations and Ono's experimental data. However, it is clear that the present experimental data agree with the results of the Kutateladze or Nishigawa correlation when the gap is larger than 20 mm for the heated plate with a diameter of 300 mm. The Kutateladze correlation agrees very well with the experimental data rather than with the Nishigawa correlation. Therefore, we can say that under the present conditions, pool boiling may be predicted by the Kutateladze correlation when the gap size is larger than 20 mm for a heated plate diameter of 300 mm. On the other hand, as clearly shown in Fig. 3(a) and (b), the heat flux for the downward case is far smaller than that for the upward case presented by Ono et al. in the same superheat condition. Therefore, the pool nucleate boiling on the downward-facing surface is weaker than that on the upward-facing surface because in the downward-facing surface case, the bubble movement may be prevented due to buoyancy and the bubbles stagnate in the gap sufficiently long that the process in which the heat is mainly transferred by latent heat transportation becomes weak.

Fig. 4 shows comparisons of the boiling curves with the heated plate diameters of 100 and 300 mm for the same approximate gap size. For the same heat flux, the results for $s = 10$ and 20 mm show the wall superheat, ΔT_{sat}, for $D = 100$ mm is smaller than that for $D = 300$ mm. That is, the larger the diameter of the stainless steel plate, the weaker the pool boiling heat transfer. This phenomenon may be explained by the bubbles under the heated plate escaping more easily to the liquid pool and churning the fluid under the heated plate more intensively. Thus, the pool boiling heat transfer with a heated plate diameter of 100 mm is stronger than that with a heated plate diameter of 300 mm under the same condition.

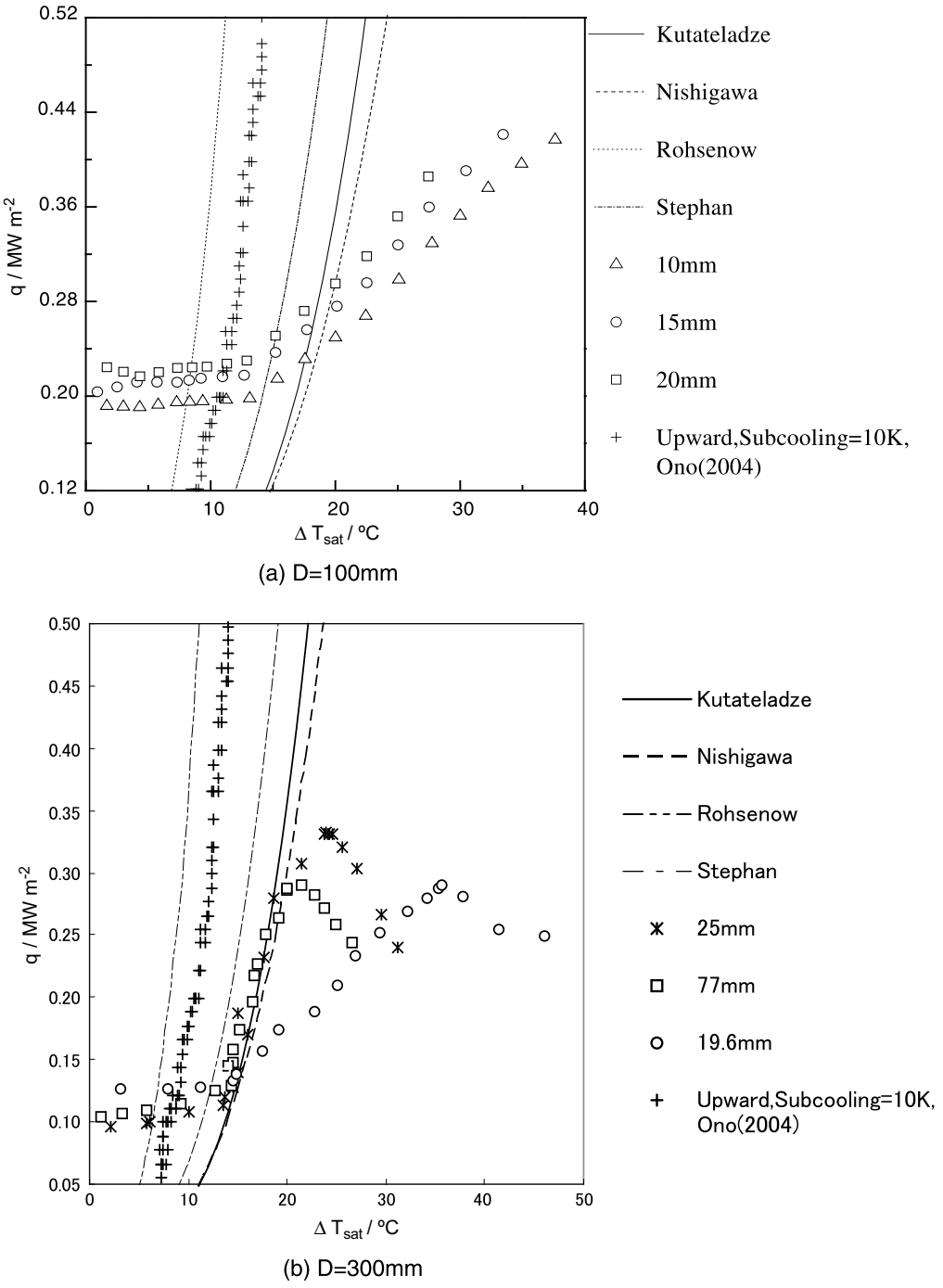

Fig. 3. Comparison of boiling curves for downward and upward-facing surfaces.

From Fig. 3(a) and (b), when the gap size is smaller than 20 mm, for either heated plate diameter, the pool boiling predicted by the correlations for an upward-facing surface is stronger than that indicated by the present experimental data. Even the results obtained by the Kutateladze correlation are larger than our experimental data. Thus, the correlations may not be used to predict pool boiling. So far there is no correlation developed to predict pool boiling on a downward-facing surface in a confined space in the open literature. In this paper, we develop a relationship as follows.

In general, the nucleate boiling for the unconfined case may be expressed by

$$q = A\Delta T_{\mathrm{sat}}^{n} \tag{4}$$

where $n = 2$–5 and A is a function of system parameters such as pressure and the properties of the working fluid.

To predict pool nucleate boiling under this condition, the confined effect should be considered. Thus, the correlation used to predict downward nucleate boiling in a confined space may be expressed by

$$q = f\left(\Delta T_{\mathrm{sat}}^{n}, Bo^{m}\right) \tag{5}$$

As discussed above, when $s > 20$ mm, the Kutateladze correlation may be directly used for the heated plate diameter of 300 mm. However, it does not fit the experimental data when $s < 20$ mm because the confined effect has not been considered. To easily obtain a new correlation, we use the experimental data from the heated

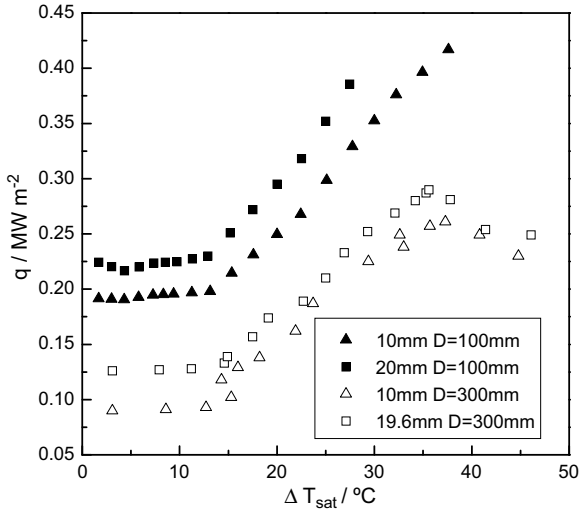

Fig. 4. Comparison of boiling curves for different diameters.

plates and then consider the effect of confinement. The Kutateladze correlation is

$$\frac{\alpha}{\lambda_f}\sqrt{\frac{\sigma}{g(\rho_f-\rho_g)}} = 7.0\times10^{-4}Pr_f^{0.35} \times\left[\frac{q_{KU}}{\rho_g h_{fg} v_f}\sqrt{\frac{\sigma}{g(\rho_f-\rho_g)}}\right]^{0.7}\left[\frac{P}{\sigma}\sqrt{\frac{\sigma}{g(\rho_f-\rho_g)}}\right]^{0.7} \quad (6)$$

where Pr_f represents the Prandtl number of saturated liquid, λ_f is the thermal conductivity of saturated liquid, W/m °C, υ_f is the kinematic viscosity of saturated liquid, m^2/s, h_{fg} is the latent heat of evaporation, J/kg, and P is the system pressure, Pa.

For each condition, the heat flux q is experimentally obtained and the heat flux q_{KU} is given by Eq. (6). Introducing the ratio of heat flux q/q_{KU} and analyzing the relationship between q/q_{KU} and the wall superheat ΔT_{sat} by the least squares method, we obtain

$$\frac{q}{q_{KU}} = C_1\Delta T_{sat}^{-2.62} \qquad \text{for } D = 100\text{ mm and } D = 300\text{ mm} \quad (7)$$

Eq. (6) gives

$$q_{KU} \propto \Delta T_{sat}^{3.33} \quad (8)$$

Thus, we have

$$q \propto \Delta T_{sat}^{0.71} \qquad \text{for } D = 100\text{ mm and } D = 300\text{ mm} \quad (9)$$

According to experimental data and using the least squares method to analyze the effect of confinement on heat transfer, we get

$$q \propto Bo^{0.1} \qquad \text{for } D = 100\text{ mm and } D = 300\text{ mm} \quad (10)$$

where Bo is the Bond number used to express the confinement level for several geometrical chambers and is defined by Eq. (1).

The bubble growth depends on not only the gap size but also the disk diameter. Therefore, another geometric scaling criterion, namely the effects of the disk diameter with respect to the bubble size, is considered in this paper. Borrowing the idea of analyzing the effect of confinement on heat transfer, a dimensionless parameter, D/L, is defined, where L is the capillary length defined by Eq. (2), to analyze the effect of the disk diameter on heat transfer. Therefore, considering the influences of wall superheat ΔT_{sat}, Bo, D/L and the properties of the working fluid λ_f, Pr_f, $\rho_g h_{fg} v_f$ and $\frac{P}{\sigma}$ and comparing the experimental data for the heated plates with the Kutateladze correlation, one can obtain a correlation by the least squares method

$$\frac{q - 95673.2Bo^{0.1} + 98241.4}{\Delta T_{sat}^{0.71}\lambda_f^{3.33}} = 1.907\times10^{-12}\left(\frac{D}{L}\right)^{0.505} Pr_f^{1.167}(\rho_g h_{fg} v_f)^{-2.333}\left(\frac{P}{\sigma}\right)^{2.333} \quad (11)$$

The relative error in Eq. (11) is defined by

$$\varepsilon = \frac{q_{EXP} - q_{CAL}}{q_{EXP}}\times 100\%$$

where q_{EXP} is the experimental heat flux and q_{CAL} is the heat flux obtained by Eq. (11). Fig. 5 shows the relative error of ±20% in Eq. (11).

3.3. Visualization

3.3.1. Bubble periodic motions

The bubble cyclic motions, shapes of coalesced bubbles, bubble sizes, and bubble period are strong functions of three important parameters. The parameters are the gap size, diameter of the heating surface, and heat flux. Even though the size of the heating surface is fixed, that is, at 100 and 300 mm for the present study, the bubble behavior can still change with gap size and heat flux. In the results mentioned previously, the maximum height of the flattened bubble is approximately 5 mm if the gap size is larger than 5 mm. That is, the bubble height will not change with the gap size changes under this condition. Furthermore, the bubble height will be same for gap sizes smaller than 5 mm. Therefore, the width of the bubbles is employed to indicate bubble size. The shapes of the bubbles likewise pertain to the width, not the height.

The boiling processes for different gap sizes are record by digital video camera from the base of the boiling surface. As an example, Fig. 6 shows a sequence of pictures taken for s = 10 mm with the heat flux increasing for D = 300 mm. From the visualization of the pool boiling phenomenon on the horizontal downward-facing surface, there are five phases for boiling that are summarized as follows:

(1) Initial phase (phase 1, Fig. 6(a)): the liquid near the heating surface is heated to a certain superheat, and the liquid directly comes into contact with the heating surface.
(2) Bubble nucleation phase (phase 2, Fig. 6(b)): if the superheat of the water near the heated surface reaches a critical value, nucleation occurs. There may be a number of very small

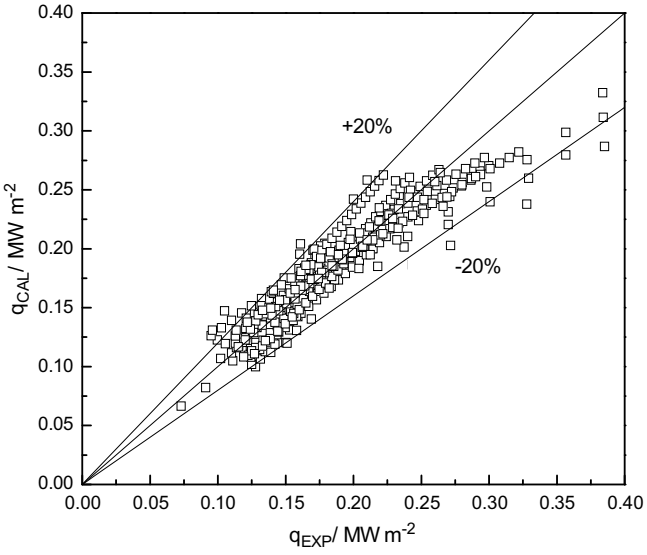

Fig. 5. Accuracy of Eq. (11).

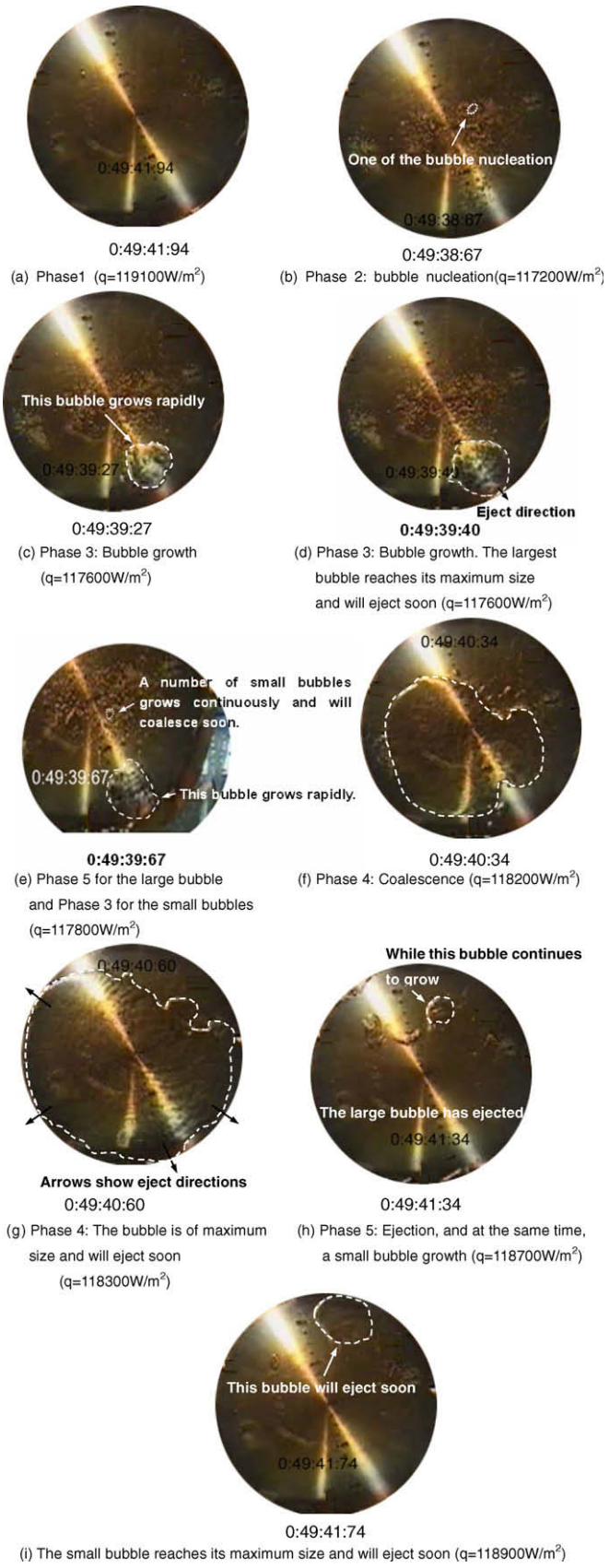

Fig. 6. Bubble circulation for $s = 10$ mm under different heat flux conditions ($D = 300$ mm).

bubbles that adhere to the boiling surface because the heated surface has a large area. Bubbles appear randomly on the heated surface.

(3) Growth phase (phase 3, Fig. 6(c)): with the continuous absorption of heat, very small bubbles grow rapidly.

(4) Bubble coalescence phase (phase 4, Fig. 6(f)): in one case, two or more neighboring bubbles come into contact with each other when their diameters reach certain values so that one or more large bubbles form. In the other case, one growing bubble coalesces with small nearby bubbles. Sometimes, the vapor mass is so large that it almost covers the entire heating surface.

(5) One or more large bubble ejection phase (phase 5, Fig. 6(h)): when one or more large bubbles reach a certain diameter, they escape from the gap to the outside. In the process of ejection, the subcooled water fills the space that was occupied by the bubble so rapidly that there is a shock effect of water on the bubble. Therefore, the coalesced bubble may be broken into vapor slugs that escape along the heated surface to the outside. If the diameter of the coalesced bubble is near that of the heated surface, the bubble motions toward the circular edge and thus it may also be broken into separate parts due to the diverging path on the heated surface and then ejected almost symmetrically to the outside. Some parts may be obstructed underneath the heated surface and then cooled by the effect of head on flowing subcooled water. In some cases, the edge of the large bubble may arrive at the edge of the heating surface in a certain direction so that it is ejected rapidly in this direction.

There are also five phases in the process of boiling for $D = 100$ mm, as for $D = 300$ mm.

Two different typical periodic bubble motions were observed in the experiments denoted as type I and type II. In general, the bubbles have the same growth process as described above for both types of periodic motion. In other words, types I and II have the same phases 1 and 2. The differences between them are in the last three phases. In phase 3, the minute bubbles simultaneously or sequentially start to grow at two or more points in the type I process; however, only one small bubble starts to grow at a certain point in the type II process. Therefore, two or more large bubbles may form in the type I process. If the large bubbles are near the periphery of the heated surface and far enough apart, two or more coalesced bubbles form; otherwise, if they are nearby, they may form one large coalesced bubble. Thus, in phase 5, one or more coalesced bubbles are ejected in the type I process, and of course only one coalesced bubble is ejected in the type II process.

This difference leads to the difference in the detail of the growing processes. The process of type II periodic motion may be clearly divided into the above five phases. However, the process of type I periodic motion is more complex. In phase 3, there are always two or more bubbles growing simultaneously. The bubble near the edge of the heated surface escapes to the outside when its edge arrives at the edge of the heated surface during its growth, while the bubbles at other locations continue to grow. Therefore, before one or more large bubbles are formed there is always a relatively small bubble that is very circular and gets ejected (Fig. 6(d) and (e)). When one or more assassinate bubbles form (phase 4), the process goes into phase 5. In the ejection process, there is always a small bubble growing (Fig. 6(h) and (i)) because the bubbles grow not only simultaneously but also continuously. Thus, after a large coalesced bubble escapes, there is another relatively small and circular bubble to be ejected. After the relatively small bubble's ejection, the process returns to phase 1 because energy accumulation is necessary to reestablish the thermal boundary layer and reheat the surface to the temperature required for the nucleation of the next bubble.

On the whole, the type I process occurs with a probability of 90.9% and the type II process occurs with a probability of 9.1% according to statistical calculations.

3.3.2. Coalesced bubble shapes

The coalesced bubbles have three kinds of shapes: circular, dumbbell-shaped and elliptical. However, most bubbles are circular. In the growth phase, the bubble remains circular. If the neighboring bubbles are very close, they may coalesce and then form a large circular bubble. If two growing bubbles are relatively far apart yet still come into contact, a dumbbell-shaped or elliptical coalesced bubble may form. When a bubble of relatively large size grows, another bubble relatively small in size may start to grow at a certain point. When the former bubble reaches its critical size, while the later bubble is still growing, it ejects in the direction of the closest point on the edge of the heated surface and there may be a suction effect on the latter bubble in the ejection direction. Therefore, the latter bubble becomes elliptical. If there are two bubbles growing simultaneously at different points, the disturbance from one bubble's growth may affect the other bubble, which would then grow into a dumbbell-shape. When one bubble moves in the ejection phase, the bubble of circular shape transforms into a dumbbell or elliptic shape due to the effect of subcooled water. The coalesced dumbbell-shaped or elliptical bubble may become circular in its growing phase.

3.3.3. Bubble size

The diameter of a coalesced bubble is relative to its position. In the process of bubble growth, if the bubble is near the edge of the heated surface, when its edge arrives at that of the heated surface, it escapes to the outside before it reaches its maximum diameter. If it is in the center of the heated surface, it may reach its maximum size and almost completely cover the heated surface. In the coalescence process for two or more large bubbles, the liquid droplets or slugs may be entrained into the large coalesced bubble. It should be noted that there may be some differences between the shapes of the bubbles in the cases of upward-facing and downward-facing boiling. In the case of horizontal upward-facing boiling, the bubble may be a sphere. In the case of horizontal downward-facing boiling, the isolated bubble may be a slightly flattened sphere if its diameter is smaller than the thickness of the gap; otherwise, it will be flat and similar to the shape of a cake with a circular arc of periphery. A coalesced bubble is always flat irrespective of whether its thickness is less than the gap size. According to our observation, the maximum thickness (height of the bubble in the vertical direction) of the coalesced bubble is approximately 5 mm. Therefore, the diameter of a bubble is defined as the maximum size in the horizontal direction that is parallel to the heating surface. Most coalesced bubble diameters are from 90 to 100 mm, that is to say, close to the diameter of the heated surface, when $D = 100$ mm, and from 100 to 200 mm, or close to the radius of heated surface, when $D = 300$ mm. Thus, the bubble diameter increases with increasing size of the heated surface. However, the increasing rate of the bubble diameter is less than that of the heated surface. That is, the increase in bubble diameter is not directly proportional to that of the heated surface.

3.3.4. Bubble ejection direction

When the relatively small coalesced bubble ejects, it always moves in one direction because the bubble is formed near the edge of the heated surface. When a large coalesced bubble ejects, there are two cases: (1) the bubble is broken into vapor slugs that are ejected in a random direction; (2) the bubble ejects in the direction of its initial motion toward the edge of the heated surface.

Underneath the heated surface, there may be from two to five bubbles that simultaneously grow and eject in a random direction because these bubbles may not coalesce trouble-free due to the effect of the liquid slugs.

3.3.5. Bubble period

In general, the bubble period is defined as the time difference for two sequential bubbles to form. However, in the present experiments, there is a new concept of period with different meaning, which may be defined as the necessary time for all the above described phases to complete. This period may be divided into two parts: the waiting time (phase 1), and the growing and escaping time (phases 2, 3, 4 and 5). According to our observation and mathematical statistics, most bubble circulation is completed within 2–10 s and the average bubble circulation period is 7 s.

4. Conclusions

From the experimental results of pool boiling on a downward-facing horizontal surface in a confined space, the main findings are as follows.

For a gap where $D = 300$ mm, pool boiling on a downward-facing surface is confined if $s < 5$ mm. The maximum confined gap size is 5 mm, which is twice the capillary length. It is semi-confined when $5\text{ mm} < s < 20$ mm and unconfined when $s > 20$ mm.

The pool boiling under the present condition is far weaker than that occurring on an upward-facing surface and the larger the diameter of the stainless steel plate, the weaker the pool boiling heat transfer. These results are predicted from the Kutateladze correlation for $s > 20$ mm, and from Eq. (11) for $s < 20$ mm.

Two kinds of bubble circulation motions were found. The typical type I motion occurs with a probability of 90.9% and the typical type II motion occurs with a probability of 9.1% according to statistical calculations. The type II bubble motion has typical five phases: (1) initial phase, (2) bubble nucleation phase, (3) growth phase, (4) bubble coalescence phase, and (5) bubble ejection phase. In type I bubble motion, phase 3 is ongoing with the escape of one mid-sized bubble; the bubble coalescence phase is more complex; and phase 5 is ongoing with the growth of a small bubble. Thus large coalesced bubbles continuously escape with the latter bubble in phase 5.

Most of the coalesced bubble diameters are from 90 to 100 mm for $D = 100$ mm and from 100 to 200 mm for $D = 300$ mm.

Acknowledgements

This work is supported by the Program for New Century Excellent Talents in University (NCET-06-0837). The financial support provided by the Japan Society for the Promotion of Science is gratefully acknowledged. The authors also acknowledge and thank Mr. H. Aoki for his assistance during the experiments.

References

Ahmed, S., Carey, V.P., 1999. Effects of surface orientation on the pool boiling heat transfer in water/2-propanol mixtures. ASME J. Heat Transfer 121, 80–88.

Bonjour, J., Lallemand, M., 1998. Flow patterns during boiling in a narrow space between two vertical surfaces. Int. J. Multiphase Flow 24, 947–960.

Bonjour, J., Lallemand, M., 2001. Two-phase flow structure near a heated vertical wall during nucleate pool boiling. Int. J. Multiphase Flow 27, 1789–1802.

Carrica, P.M., Leonardi, S.A., Clausse, A., 1995. Experimental study of the two-phase flow dynamics in nucleate and film pool boiling. Int. J. Multiphase Flow 21, 405–418.

Cheung, F.B., Haddad, K.H., Liu, Y.C., 1999. Boundary layer boiling and critical heat flux phenomena on a downward facing hemispherical surface. Nucl. Technol. 126, 243–264.

Chu, T.Y., Bainbridge, B.L., Simpson, R.B., Bentz, J.H., 1997. Ex-vessel boiling experiments: laboratory- and reactor-scale testing of the flooded cavity concept for in-vessel core retention. Part I. Observation of quenching of downward-facing surfaces. Nucl. Eng. Des. 169, 77–88.

El-genk, M.S., Bostanci, H., 2003. Combined effects of subcooling and surface orientation on pool boiling of HFE-7100 from a simulated electronic chip. Exp. Heat Transfer 16, 281–301.

El-genk, M.S., Gao, C., 1999. Experiments on pool boiling of water from downward facing hemispheres. Nucl. Technol. 125, 52–69.
El-genk, M.S., Glebov, A.G., 1995. Transient pool boiling from downward facing curved surface. Int. J. Heat Mass Transfer 38, 2209–2224.
El-genk, M.S., Glebov, A.G., 1996. Film boiling from a downward facing curved surface in saturated and subcooled water. Int. J. Heat Mass Transfer 39, 275–288.
Haddad, K.H., Cheung, F.B., 1998. Steady-state subcooling nucleate boiling on a downward facing hemispherical surface. Trans. ASME J. Heat Transfer 120, 365–370.
Hetsroni, G., Gurevich, M., Mosyak, A., Rozenblit, R., Yarin, L.P., 2002. Subcooled boiling of surfactant solutions. Int. J. Multiphase Flow 28, 347–361.
Katto, Y., Yokoya, S., Teraoka, K., 1977. Nucleate and transition boiling in a narrow space between two horizontal, parallel disk surface. Bull. JSME 20, 638–643.
Kim, H.J., Jeong, J.H., 2006. Numerical analysis of experimental observations for heat transfer augmentation by ultrasonic vibration. Heat Transfer Eng. 27, 14–22.
Kim, J., Kim, M.H., 2006. On the departure behaviors of bubble at nucleate pool boiling. Int. J. Multiphase Flow 32, 1269–1286.
Kim, Y.H., Suh, K.Y., 2003. One-dimensional critical heat flux concerning surface orientation and gap size effects. Nucl. Eng. Des. 226, 277–292.
Kim, Y.H., Kim, S.J., Kim, J.J., Noh, S.W., Suh, K.Y., Rempe, J.L., Cheung, F.B., Kim, S.B., 2005. Visualization of boiling phenomena in inclined rectangular gap. Int. J. Multiphase Flow 31, 618–642.
Kim, J., Oh, B.D., Kim, M.H., 2006. Experimental study of pool temperature effects on nucleate pool boiling. Int. J. Multiphase Flow 32, 208–231.
Kutateladze, S.S., 1952. Heat transfer in condensation and boiling. USAEC Report AEC-tr-3770.
Lee, H.C., Oh, B.D., Bae, S.W., Kim, M.H., 2003. Single bubble growth in saturated pool boiling on a constant wall temperature surface. Int. J. Multiphase Flow 29, 1857–1874.
Lee, S.D., Lee, J.K., Suh, K.Y., 2007. Natural convection thermo fluid dynamics in a volumetrically heated rectangular pool. Nucl. Eng. Des. 237, 473–483.
Nishigawa, K., Fujita, Y., 1977. Correlation of nucleate boiling heat transfer based on bubble population density. Int. J. Heat Mass Transfer 22, 233–245.
Nishigawa, K., Fujita, Y., Uchida, S., Ohta, H., 1984. Effect of configuration on nucleate boiling heat transfer. Int. J. Heat Mass Transfer 27, 1559–1571.
Nomura, S., Yamamoto, A., Murakami, K., 2002. Ultrasonic heat transfer enhancement using a horn-type transducer. Jpn. J. Appl. Phys. 1 41, 3217–3222.
Ono, A., Sakashita, H., 2004. Liquid vapor structure near heating surface at high heat flux in subcooled pool boiling. Trans. Jpn. Soc. Mech. Eng. B 70, 2951–2958 (in Japanese).
Passos, J.C., Hirata, F.R., Possamai, L.F.B., Balsamo, M., Misale, M., 2004. Confined boiling of FC72 and FC87 on a downward facing heating copper disk. Int. J. Heat Fluid Flow 25, 313–319.
Phanikumar, M.S., Mahajan, R.L., 1998. Numerical analysis of unsteady thermosolutal convection over a horizontal isothermal circular cylinder. Numer. Heat Transfer A 33, 673–700.
Prakash Narayan, G., Anoop, K.B., Sateesh, G., Sarit, K.D., 2008. Effect of surface orientation on pool boiling heat transfer of nanoparticle suspensions. Int. J. Multiphase Flow 34, 145–160.
Radziemska, E., Lewandowski, W.M., 2001. Heat transfer by natural convection from an isothermal downward-facing round plate in unlimited space. Appl. Energy 68, 347–366.
Rohsenow, W.M., 1952. A method of correlating heat transfer data for surface boiling of liquids. Trans. ASME 74, 969–976.
Stephan, K., Abdelsalam, M., 1980. Heat-transfer correlations for natural convection boiling. Int. J. Heat Mass Transfer 23, 73–87.
Su, G.H., Sugiyama, K., 2007. Natural convection heat transfer of water on a horizontal downward facing stainless steel disk in a gap under atmospheric pressure conditions. Ann. Nucl. Energy 34, 93–102.
Su, G.H., Fukuda, K., Morita, K., 2002a. Applications of artificial neural network for the prediction of pool boiling curves. In: Proceedings of the 10th International Conference on Nuclear Engineering (ICONE10), Washington, USA, ICONE10-22487.
Su, G.H., Fukuda, K., Morita, K., et al., 2002b. Applications of artificial neural network for the prediction of flow boiling curves. J. Nucl. Sci. Technol. 39, 1190–1198.
Wolf, J.R., Alers, D.W., Neimark, L.A., 1994. Relocation of molten material to the TMI-2 lower head. Nucl. Safety 35, 269–279.
Yang, S.H., Baek, W.P., Chang, S.H., 1997. Pool boiling critical heat flux of water on small plates: effects of surface orientation and size. Int. Commun. Heat Mass Transfer 24, 1093–1102.
Yang, J., Dizon, M.B., Cheung, E.B., Rempe, J.L., Suh, K.Y., Kim, S.B., 2005. Critical heat flux for downward facing boiling on a coated hemispherical surface. Exp. Heat Transfer 18, 223–242.
Yao, S.C., Chang, Y., 1983. Pool boiling heat transfer in a confined space. Int. J. Heat Mass Transfer 26, 841–848.
Yoon, H.Y., Koshizuka, S., Oka, Y., 2001. Direct calculation of bubble growth, departure, and rise in nucleate pool boiling. Int. J. Multiphase Flow 27, 277–298.